SAND2008-3074C

YUCCA MOUNTAIN 2008 PERFORMANCE ASSESSMENT: UNCERTAINTY AND SENSITIVITY ANALYSIS FOR PHYSICAL PROCESSES

C. J. Sallaberry, A. Aragon , A. Bier, Y. Chen, J.W. Groves, C.W. Hansen, J.C. Helton, S. Mehta, S.P. Miller, J. Min, P. Vo

Sandia National Laboratories, Albuquerque, NM 87185-0776, cnsalla@sandia.gov

The 2008 performance assessment (PA) for the proposed high level radioactive waste repository at Yucca Mountain, Nevada, uses a sampling-based approach to uncertainty and sensitivity analysis. Specifically, Latin hypercube sampling is used to generate a mapping between epistemically uncertain analysis inputs and analysis outcomes of interest. This results in distributions that characterize the uncertainty in analysis outcomes. Further, the resultant mapping can be explored with sensitivity analysis procedures based on (i) examination of scatterplots, (ii) partial rank correlation coefficients, (iii) R^2 values and standardized rank regression coefficients obtained in stepwise rank regression analyses, and (iv) other procedures. The 2008 YM TSPA (Total System Performance Assessment) considers over 300 epistemically uncertain inputs (e.g., corrosion properties, solubilities, retardations, defining parameters for Poisson processes, ...) and over 70 time-dependent analysis outcomes (e.g., physical properties in waste packages and the engineered barrier system, releases from the engineered barrier system, the unsaturated zone and the saturated zone for individual radionuclides, and annual dose to the reasonably maximally exposed individual (RMEI) from both individual radionuclides and all radionuclides. The obtained uncertainty and sensitivity analysis results play an important role in facilitating understanding of analysis results, supporting analysis verification, establishing risk importance, providing guidance for future model development and data acquisition, and enhancing overall analysis credibility. The uncertainty and sensitivity analysis procedures are illustrated and explained with selected results for releases from the engineered barrier system, the unsaturated zone and the saturated zone and also for annual dose to the RMEI.

I. INTRODUCTION

The importance of an appropriate assessment of uncertainty present in performance assessments (PAs) for the proposed Yucca Mountain (YM) repository for high-level radioactive waste has been strongly emphasized by the U.S. Nuclear Regulatory Commission (NRC) (e.g., Ref. 1, Quotes (NRC4) and (NRC5)). As a result, uncertainty analysis and sensitivity analysis are important parts of the YM 2008 PA, where uncertainty analysis designates the determination of the uncertainty in analysis results that derives from uncertainty in analysis inputs and sensitivity analysis designates the determination of the contributions of individual uncertain analysis inputs to the uncertainty in analysis results.

As described in a preceding presentation [1] and in more detail in an extensive analysis report ([2], App. J), the conceptual structure and computational organization of the YM 2008 PA involves three basic entities: (EN1) a characterization of the uncertainty in the occurrence of future events that could affect the performance of the repository; (EN2) models for predicting the physical behavior and evolution of the repository; and (EN3) a characterization of the uncertainty associated with analysis inputs that have fixed but imprecisely known values. The designators aleatory and epistemic are commonly used for the uncertainties characterized by entities (EN1) and (EN3), respectively. Formally, (EN1) is defined by a probability space $(\mathcal{A}, A, p_A)$ ([1], Sect. III); (EN2) corresponds to a very complex function that predicts the time-dependent behavior of many different physical properties associated with the evolution of the YM repository system ([3-5]; [2], Chap. 6); and (EN3) is defined by a probability space $(\mathcal{E}, E, p_E)$ ([1], Sect. III).

In the context of the preceding entities, uncertainty analysis involves the determination of the uncertainty in predictions by the model that corresponds to (EN2) that derives from the uncertainty in analysis inputs characterized by the probability space $(\mathcal{E}, E, p_E)$. Further, this determination is made for either (i) results conditional on the occurrence of specific futures contained in the set $\mathcal{A}$ (see [1], Table I) or (ii) expected results based on the probability space $(\mathcal{A}, A, p_A)$ and obtained by integrating over the set $\mathcal{A}$ (see [1], Sect. IV). Similarly, sensitivity analysis involves the determination of the effects of individual variables contained in elements $\mathbf{e}$ of $\mathcal{E}$ (see [1], Table II) on results of the form just indicated.

The primary emphasis of this presentation is on uncertainty and sensitivity analysis for results conditional on the occurrence of specific futures contained in the set $\mathcal{A}$. A following presentation considers uncertainty and

sensitivity analysis for expected results based on the probability space ($\mathcal{A}$, A, p_A) and obtained by integrating over the set $\mathcal{A}$ [6].

II. UNCERTAINTY AND SENSITIVITY ANALYSIS

Conceptually, the component (EN2) of the YM 2008 PA can be represented by a function

$$\mathbf{y}(\tau \mid \mathbf{a},\mathbf{e}) = \mathbf{f}(\tau \mid \mathbf{a},\mathbf{e}), \quad (1)$$

where

$$\mathbf{a} = [a_1, a_2, ..., a_{nA}] \quad (2)$$

is an element (i.e., future) contained in $\mathcal{A}$ (see [1], Table I),

$$\mathbf{e} = [e_1, e_{2,...,} e_{nE}] \quad (3)$$

is an element of $\mathcal{E}$ (see [1], Eq. (4) and Table II), and

$$\mathbf{y}(\tau \mid \mathbf{a},\mathbf{e}) = [y_1(\tau \mid \mathbf{a},\mathbf{e}), y_2(\tau \mid \mathbf{a},\mathbf{e}), ..., y_{nY}(\tau \mid \mathbf{a},\mathbf{e})] \quad (4)$$

is the value of the function $\mathbf{f}(\tau \mid \mathbf{a},\mathbf{e})$ at time τ (see [3-5]; [2], Chap. 6). In general, the dimensions nA and nY of $\mathbf{a}$ and $\mathbf{y}(\tau \mid \mathbf{a},\mathbf{e})$ can be quite large. Further, the dimension nE of $\mathbf{e}$ in the YM 2008 PA is 392; however, most elements of $\mathbf{y}(\tau \mid \mathbf{a},\mathbf{e})$ are potentially affected by only a subset of the variables contained in $\mathbf{e}$. The elements of $\mathbf{y}(\tau \mid \mathbf{a},\mathbf{e})$ include both physical properties of the YM system (e.g., temperature, pH, radionuclide release rates, …) and quantities involving dose to the reasonably maximally exposed individual (RMEI) (e.g., the doses $D_N(\tau \mid \mathbf{a}_N,\mathbf{e})$, $D_C(\tau \mid \mathbf{a},\mathbf{e})$ and $D(\tau \mid \mathbf{a},\mathbf{e})$ discussed in Sects. IV and V of Ref. [1] are elements of $\mathbf{y}(\tau \mid \mathbf{a},\mathbf{e})$).

The uncertainty associated with $\mathbf{e}$ is characterized by a sequence of distributions

$$D_1, D_2, ..., D_{nE}, \quad (5)$$

where D_j is the distribution assigned to the element e_j of $\mathbf{e}$ (i.e., see the variables and distributions indicated in Table II of Ref. [1] and given in full in Tables K3-1, K3-2 and K3-3 of Ref. [2]). Correlations and other restrictions are also assumed to exist between some variables. The distributions indicated in Eq. (5) and any associated restrictions characterize epistemic uncertainty and, in effect, define the probability space ($\mathcal{E}$, E, p_E).

Latin hypercube sampling [7,8] is used to propagate the uncertainty characterized by the distributions indicated in Eq. (5) through the YM 2008 PA. Specifically, a Latin hypercube sample (LHS)

$$\mathbf{e}_i = [e_{i1}, e_{i2}, \cdots, e_{inE}], \; i = 1,2,\cdots,n, \quad (6)$$

of size n = 300 is generated from the possible values for $\mathbf{e}$ (i.e., form the set $\mathcal{E}$). Then, the function $\mathbf{f}(\tau \mid \mathbf{a},\mathbf{e})$ is evaluated for each element $\mathbf{e}_i$ of the LHS indicated in Eq. (6). This creates a mapping

$$[\mathbf{e}_i, \mathbf{y}(\tau \mid \mathbf{a}, \mathbf{e}_i)], \; i = 1,2,\cdots,n = 300, \quad (7)$$

from uncertain analysis inputs to uncertain analysis results. In practice, the indicated mapping is generated many times for different values of $\mathbf{a}$ for the calculation of each of the doses $D_C(\tau \mid \mathbf{a},\mathbf{e})$ indicated in Table III of [1]).

Once generated, the mapping in Eq. (7) provides the basis for both uncertainty analysis and sensitivity analysis. Specifically, each sample element has a weight (i.e., a probability in common but incorrect usage) of 1/n = 1/300 that can be used to construct cumulative distribution functions (CDFs) and complementary cumulative distribution functions (CCDFs) that summarize the uncertainty in analysis results. In addition, expected values (i.e., means) and various quantiles can also be obtained and used to summarize the uncertainty in analysis results. Or, most simply, the spread of the results obtained for individual elements of $\mathbf{y}(\tau \mid \mathbf{a},\mathbf{e})$ can be presented.

Sensitivity analysis results can be obtained by exploring the mapping between analysis inputs and analysis results in Eq. (7) with a variety of procedures. The simplest is to examine scatterplots that graphically show the relationship between an element of $\mathbf{y}(\tau \mid \mathbf{a},\mathbf{e})$ and individual elements of $\mathbf{e}$ (i.e., plots of points of the form [e_{ij}, $\mathbf{y}_k(\tau \mid \mathbf{a},\mathbf{e}_i)$], i = 1, 2, …., n, for individual elements e_j and $\mathbf{y}_k(\tau \mid \mathbf{a},\mathbf{e})$ of $\mathbf{e}$ and $\mathbf{y}(\tau \mid \mathbf{a},\mathbf{e})$, respectively). More complex analyses involve the use of partial correlation coefficients (PCCs) and stepwise regression analyses to assess the relationships between analysis inputs and analysis results. With stepwise regression analysis, variable importance is indicated by the order of selection in the stepwise process, the incremental increase in R^2 values as variables are added to the regression model, and the standardized regression coefficients (SRCs) in the final regression model. A SRC provides a measure of the fraction of the uncertainty in an analysis accounted for by a given analysis input; in contrast, a PCC provides a measure of the strength of the linear relationship between an analysis result and a given analysis input after the linear effects of all other analysis inputs have been removed. When nonlinear relationships

are present, analyses are often performed with rank transformed data, which results in partial rank correlation coefficients (PRCCs) and standardized rank regression coefficients (SRRCs) rather than PCCs and SRCs.

Additional information on the sampling based uncertainty and sensitivity analysis procedures used in the YM 2008 PA is available in a recent review article [9].

III. NOMINAL SCENARIO CLASS $\mathcal{A}_N$

A large number of analysis results are considered in the uncertainty and sensitivity analyses for the nominal scenario class $\mathcal{A}_N$ (Table I). The variables indicated in Table I correspond to a subset of the variables $\mathbf{y}_k(\tau \mid \mathbf{a}, \mathbf{e})$ that comprise the elements of $\mathbf{y}(\tau \mid \mathbf{a}, \mathbf{e})$ in Eq. (4). Of these variables, the number of failed commercial spent nuclear fuel waste packages in percolation bin 3 (*NCSFL*) is used as an initial example for illustration (Fig. 1). The element $\mathbf{a}_N$ of $\mathcal{A}$ under consideration corresponds to the future in which no disruptions of any kind take place.

TABLE I. Examples of 11 of the 32 Time-Dependent Results Analyzed for Nominal Scenario Class ([2], Table K4.1-1)

BACSFLAD : Average breached area (m^2) on failed CSNF WPs under dripping conditions ([2], Figures K.4.2-6, K.4.2-7)
DOSTOT: Dose to RMEI (mrem/yr) from all radioactive species ([2], Figures K4.5-1, K4.5-2, K4.5-3)
DSFLTM : Drip Shield failure time (yr) ([2], Figure K.4.2-1)
ISCSINAD : Ionic strength (molal) in the invert beneath the WP for CSNF WPs under dripping conditions ([2], Figures K.4.3-9, K.4.3-11)
NCDFL : Number of failed CDSP WPs ([2], Figure K.4.2-2)
NCSFL : Number of failed CSNF WPs ([2], Figures K.2-1, K.4.2-3)
NCSFLAD : Number of failed CSNF WPs under dripping conditions ([2], Figures K.4.2-4, K.4.2-5)
NCSFLND : Number of failed CSNF WPs under nondripping conditions ([2], Figures K.4.2-4, K.4.2-5)
PCO2CSIA : Partial pressure of CO_2 (bars) in the invert for CSNF WPs under dripping conditions ([2], Figures K.4.3-7, K.4.3-8)
PHCSINAD : pH in the invert beneath the WP for CSNF WPs under dripping conditions ([2], Figures K.4.3-12, K.4.3-13)
RHCDINV : Relative humidity for CDSP WPs in the invert beneath the WP ([2], Figure K.4.3-6)

(a)

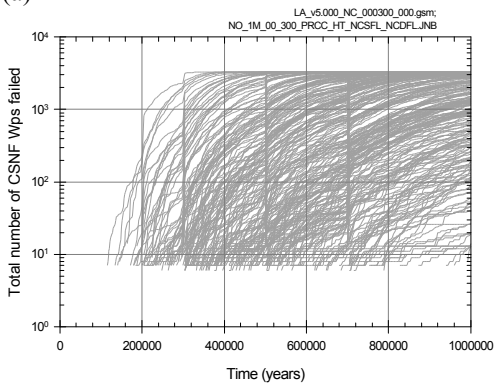

(b)

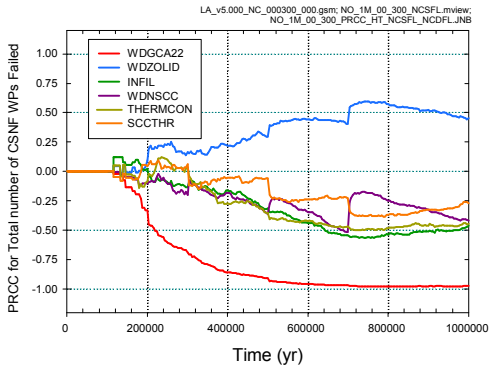

(c)

NCSFL: 1M yr		
Variable[a]	**R^2 [b]**	**SRRC[c]**
WDGCA22	0.91	-0.98
WDZOLID	0.92	0.10
INFIL	0.93	-0.12
THERMCON	0.94	-0.10
WDNSCC	0.95	-0.09
WDGCUA22	0.96	0.09
SCCTHR	0.96	-0.05

(d)

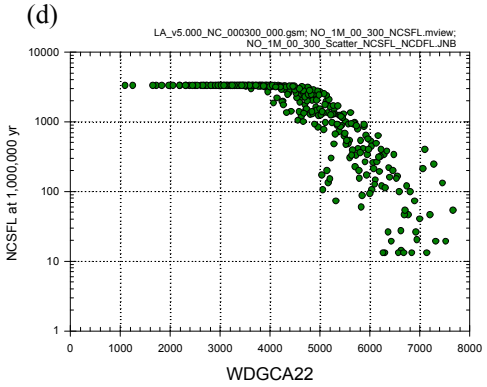

a: Variables listed in order of selection in stepwise regression
b: Cumulative R^2 value with entry of each variable into regression model
c: SRRCs in final regression model

Fig. 1. Uncertainty and sensitivity analysis results for *NCSFL*: (a) *NCSFL* for all (i.e., 300) sample elements, (b) PRCCs for *NCSFL*, (c) stepwise rank regression analysis for *NCSFL* at 10^6 yr, and (d) scatterplot for (*WDGCA22, NCSFL*) at 10^6 yr ([2], Fig. K2-1)

The uncertainty in the time dependent values for *NCSFL* is shown by the 300 curves in Fig. 1a, with a single curve resulting for each of the LHS elements $\mathbf{e}_i$ in Eq. (6). Sensitivity analysis results based on PRCCs and stepwise rank regression are presented in Figs. 1b and 1c. In both analyses, the dominant variable with respect to the uncertainty in *NCSFL* is *WDGCA22* (see Table II for variable definitions), with *NCSFL* tending to decrease as *WDGCA22* increases. This effect results because of the role that increasing *WDGCA22* plays in decreasing the rate of general corrosion. The strong effect of *WDGCA22* on *NCSFL* can be seen in the scatterplot in Fig. 1d. After *WDGCA22*, a number of additional variables are identified as having small effects on *NCSFL*.

TABLE II. Variables Appearing in Sensitivity Analyses for *NCSFL* and *DOSTOT* in Figs. 1 and 2 ([2], Tables K3-1, K3-2, K3-3)

WDGCA22: Temperature dependent slope term of Alloy 22 general corrosion rate (K).
WDZOLID : Deviation from median yield strength range for outer lid (dimensionless).
INFIL : Pointer variable for determining infiltration conditions: 10^{th}, 30^{th}, 50^{th} or 90^{th} percentile infiltration scenario (dimensionless).
THERMCON : Selector variable for one of three host-rock thermal conductivity scenarios (low, mean, and high) (dimensionless).
WDNSCC : Stress corrosion cracking growth rate exponent (repassivation slope) (dimensionless).
WDGCUA22: Variable for selecting distribution for general corrosion rate (low, medium, or high) (dimensionless).
SCCTHR : Stress threshold for stress corrosion cracking (MPa).

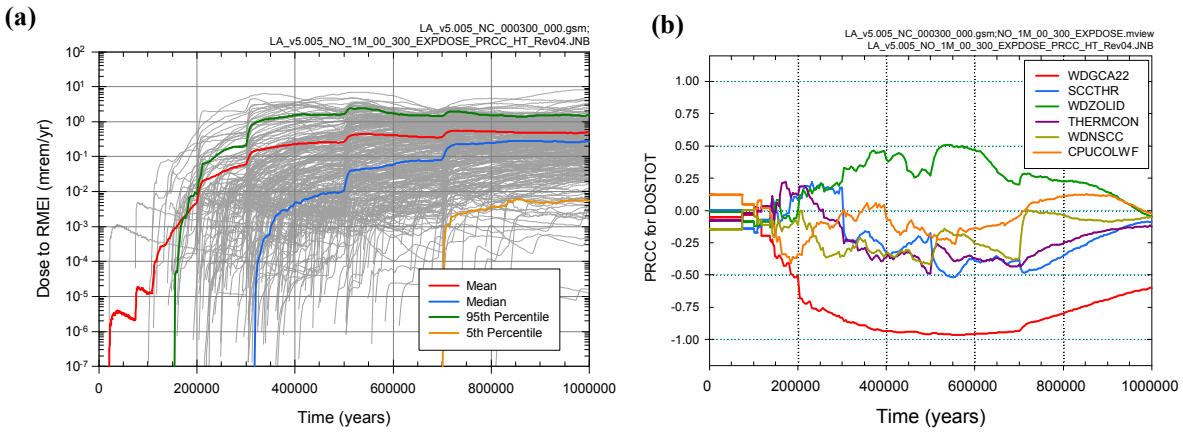

Fig. 2. Uncertainty and sensitivity analysis results for *DOSTOT* (i.e., for $D_N(\tau \mid \mathbf{a}_N, \mathbf{e}_M)$ as defined in Table III of Ref. [1]): (a) *DOSTOT* for all (i.e., 300) sample elements, and (b) PRCCs for *DOSTOT* ([2], Fig. K4.5-1[a]).

As another example, analyses for dose from all radionuclides for the nominal scenario class $\mathcal{A}_N$ (i.e., $D_N(\tau \mid \mathbf{e}_M)$, or equivalently, *DOSTOT*) are presented in Fig. 2. The uncertainty in the time dependent values for *DOSTOT* is shown by the 300 curves in Fig. 2a, with a single curve resulting for each of the LHS elements $\mathbf{e}_i$ in Eq. (6). Sensitivity analysis results based on PRCCs are presented in Fig. 2b. The dominant variables with respect to the uncertainty in *DOSTOT* are *WDGCA22* and *WDZOLID* (see Table II for variable definitions), with *DOSTOT* tending to decrease as *WDGCA22* increases and to increase as *WDZOLID* as increases. These effects result because increasing *WDGCA22* decreases WP failures due to general corrosion (see Fig. 1) and increasing *WDZOLID* increases corrosion-induced failures of welds at the WP lids.

Analyses similar to those presented in Figs. 1 and 2 were carried out for the nominal scenario class for all 32 analysis results indicated in Table I ([2], Sect. K4).

IV. IGNEOUS INTRUSIVE SCENARIO CLASS $\mathcal{A}_{II}$

As for the nominal scenario class, a large number of analysis results are considered in the uncertainty and sensitivity analyses for the igneous scenario class $\mathcal{A}_{II}$ (Table III). The variables indicated in Table III correspond to a subset of the variables $\mathbf{y}_k(\tau \mid \mathbf{a}, \mathbf{e})$ that comprise the elements of $\mathbf{y}(\tau \mid \mathbf{a}, \mathbf{e})$ in Eq. (4). As examples, this section considers the movement of ^{237}Np

through the repository system and the dose to the RMEI that results from this movement. The specific element **a** of $\mathcal{A}$ under consideration corresponds to a single igneous intrusive event that occurs at 10 yr after repository closure and damages all waste packages in the repository, and the results selected for use are *ESNP237*, *UZNP237*, *SZNP237* and *DONP237* as defined in Table III.

TABLE III. Examples of 7 of the 49 Time-Dependent Results Analyzed for Igneous Intrusive Scenario Class ([2], Table K6.1-1)

DONP237: Dose to RMEI (mrem/yr) from dissolved ^{237}Np ([2], Figures K.6.6.1-5, K.6.6.1-6, K.6.6.2-3)
ESNP237: Release rate (g/yr) for the movement of dissolved ^{237}Np from the EBS to the UZ ([2], Figures K.6.3.1-5, K.6.3.1-6, K.6.3.2-3)
ESNP237C : Cumulative release (g) for the movement of dissolved ^{237}Np from the EBS to the UZ ([2], Figures K.6.3.1-5, K.6.3.1-6, K.6.3.2-3, K.6.4.1-9)
SZNP237: Release rate (g/yr) for the movement of dissolved ^{237}Np across a subsurface plane at the location of the RMEI ([2], Figures K.6.5.1-7, K.6.5.1-8, K.6.5.2-3)
SZNP237C : Cumulative release (g) for the movement of dissolved ^{237}Np across a subsurface plane at the location of the RMEI ([2], Figures K.6.5.1-7, K.6.5.1-8, K.6.5.1-9, K.6.5.2-3)
UZNP237: Release rate (g/yr) for the movement of dissolved ^{237}Np from the UZ to the SZ ([2], Figures K.6.4.1-7, K.6.4.1-8)
UZNP237C : Cumulative release (g) for the movement of dissolved ^{237}Np from the UZ to the SZ ([2], Figures K.6.4.1-7, K.6.4.1-8, K.6.4.1-9, K.6.5.1-9)

The uncertainty in the time-dependent values for *ESNP237* and *UZNP237* are shown by the 300 curves in Figs. 3a and 3c, with a single curve resulting for each of the LHS elements $\mathbf{e}_i$ in Eq. (6). Sensitivity analysis results for *ESNP237* based on PRCCs are presented in Fig. 3b and indicate (i) positive effects for *EP1NPO2, INFIL, DELPPCO2* and *EP1LOWAM*, (ii) a negative effect for *PHCSS*, and (iii) a very early positive effect for *THERMCON* (see Table IV for variable definitions). The indicated effects result because (i) increasing *EP1NPO2* and *DELPPCO2* increases the solubility of neptunium, (ii) increasing *INFIL* increases water flow through the EBS, (iii) increasing *EP1LOWAM* increases the solubility of ^{241}Am, which is a parent of ^{237}Np, (iv) increasing *PHCSS* decreases the solubility of neptunium, and (v) increasing *THERMCON* decreases the time required for the repository to reach below-boiling temperatures for water and thereby facilitates early radionclide releases.

(a)

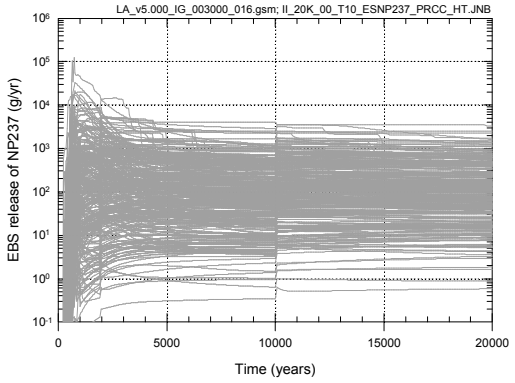

(b)

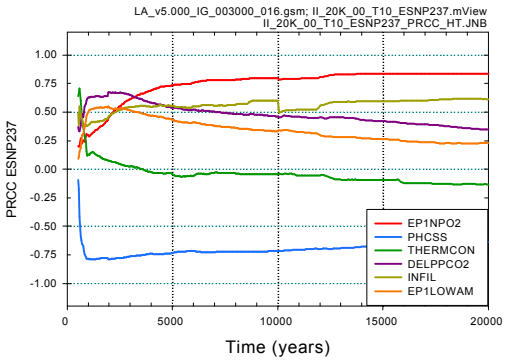

(c)

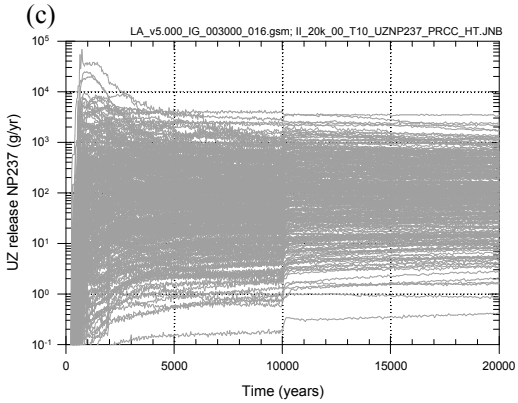

(d)

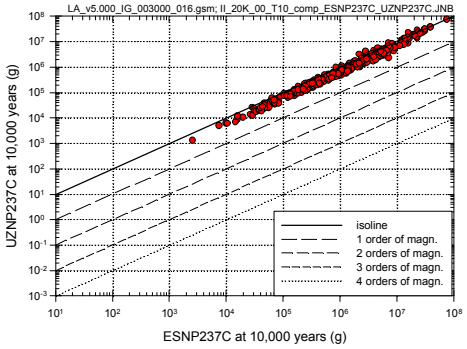

Fig. 3. Uncertainty and sensitivity analysis results for *ESNP237* and *UZNP237*: (a) *ESNP237* for all (i.e., 300) sample elements, (b) PRCCs for *ESNP237*, (c) *UZNP237* for all (i.e., 300) sample elements, and (d) scatterplot for (*ESNP237C*, *UZNP237C*) at 10^4 yr ([2], Figs. K6.3.1-5, K6.4.1-7, and K6.4.1-9)

TABLE IV. Variables Appearing in Sensitivity Analyses for *ESNP237* and *SZNP237* in Figs. 3 and 4 ([2], Tables K3-1, K3-2, K3-3)

EP1NPO2: Logarithm of the scale factor used to characterize uncertainty in NpO_2 solubility at an ionic strength below 1 molal (dimensionless).
PHCSS: Pointer variable used to determine pH in CSNF Cell1 under liquid influx conditions (dimensionless).
THERMCON: Selector variable for one of three host-rock thermal conductivity scenarios (low, mean, and high) (dimensionless).
DELPPCO2: Selector variable for partial pressure of CO_2 (dimensionless).
INFIL: Pointer variable for determining infiltration conditions: 10^{th}, 30^{th}, 50^{th} or 90^{th} percentile infiltration scenario (dimensionless).
EP1LOWAM: Logarithm of the scale factor used to characterize uncertainty in americium solubility at an ionic strength below 1 molal (dimensionless).
SZGWSPDM: Logarithm of the scale factor used to characterize uncertainty in groundwater specific discharge (dimensionless).
SZFIPOVO: Logarithm of flowing interval porosity in volcanic units (dimensionless).

The comparison of the cumulative releases *ESNP237C* and *UZNP237C* at 10^4 yr in the scatterplot in Fig. 3d shows that the processes in the unsaturated zone have little effect on the uncertainty in the movement of ^{237}Np. As a result, the unpresented PRCCs for *UZNP237* are essentially the same as the PRCCs for *ESNP237* in Fig. 3b.

The uncertainty in the time dependent values for *SZNP237* and *DONP237* are shown by the 300 curves in Figs. 4a and 4c. Unlike the unsaturated zone, the saturated zone can have a significant effect on the movement of ^{237}Np to the location of the RMEI (Fig. 5).

Sensitivity analysis results for *ESNP237* based on PRCCs are presented in Fig. 4b and indicate (i) positive effects for *SZGWSDM*, *EP1NPO2* and *INFIL,* (ii) a negative effect for *PHCSS*, and (iii) an early positive effect *THERMCON* and a early negative effect for *SZFIPOVO* (see Table IV for variable definitions). The indicated effects for *EP1NPO2*, *INFIL* and *PHCSS* derive from their previously discussed effects on release from the EBS. The positive effect associated with *SZGWSDM* results from increasing water flow in the SZ, and the early negative effect associated with *SZFIPOVO* results from slowing the initial movement of released radionuclides in the SZ.

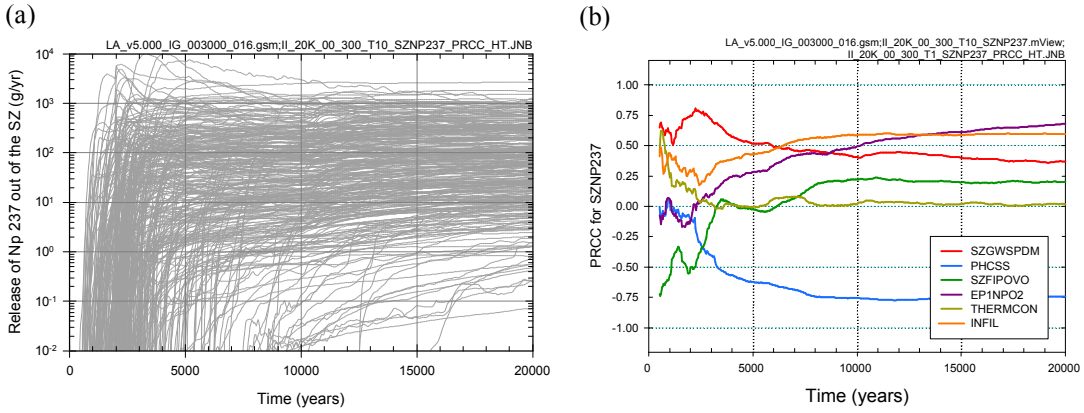

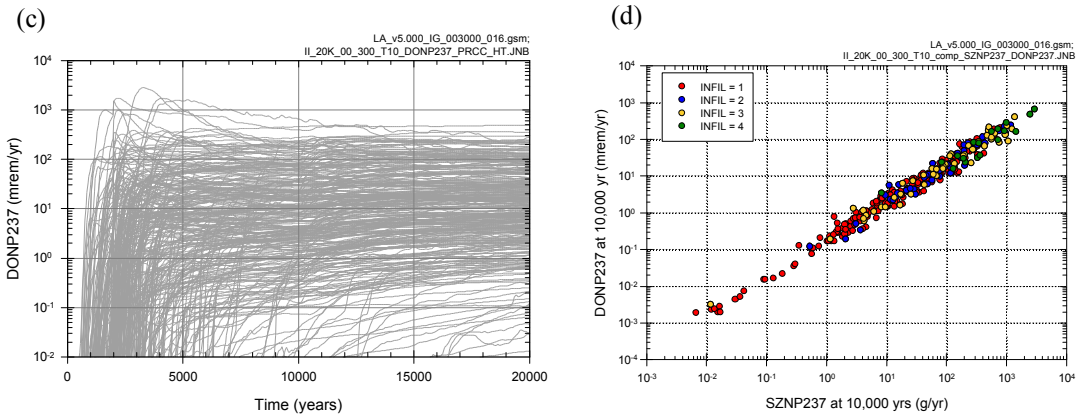

Fig. 4. Uncertainty and sensitivity analysis results for *SZNP237* and *DONP237*: (a) *SZNP237* for all (i.e., 300) sample elements, (b) PRCCs for *SZNP237*, (c) *DONP237* for all (i.e., 300) sample elements, and (d) scatterplot for (*SZNP237*, *DONP237*) at 10^4 yr ([2], Figs. K6.5.1-7, K6.6.1-5 and K6.6.1-6).

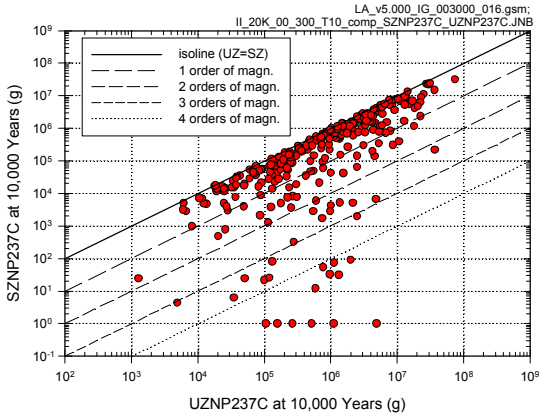

Fig. 5. Scatterplot for (*UZNP237C*, *SZNP237C*) at 10^4 yr ([2], Fig. K6.5.1-9).

The comparison of *SZNP237* and *DONP237* at 10^4 yr in the scatterplot in Fig. 4d shows that the uncertainty in *SZNP237* dominates the uncertainty in *DONP237*. As a result, the unpresented PRCCs for *DONP237* are essentially the same as the PRCCs for *SZNP237* in Fig. 4b.

Analyses similar to those presented in Figs. 3-5 were carried out for all 49 analysis results indicated in Table I ([2], Sect. K6).

V. ADDITIONAL SCENARIO CLASSES

Example uncertainty and sensitivity analysis results have been presented for the nominal scenario class $\mathcal{A}_N$ and the igneous intrusive scenario class $\mathcal{A}_{II}$. In addition, extensive uncertainty and sensitivity analyses were also carried out as part of the YM 2008 PA for the early waste package failure scenario class $\mathcal{A}_{EW}$, the early drip shield failure scenario class $\mathcal{A}_{ED}$, the igneous eruptive scenario class $\mathcal{A}_{IE}$, the seismic ground motion scenario class $\mathcal{A}_{SG}$, and the seismic fault displacement scenario class $\mathcal{A}_{SF}$. In performing these analyses, two different time periods were considered for the definition of the sample space $\mathcal{A}$ for aleatory uncertainty: $[0, 2\times10^4$ yr] and [0, 10^6 yr]. The results of these analyses are given in Apps. J and K of Ref. [2].

V. SUMMARY

The importance of an appropriate assessment of the uncertainty present in PAs for the proposed YM repository for high-level radioactive waste has been strongly emphasized by the NRC (e.g., [1], Quotes (NRC4) and (NRC5)). In response, extensive sampling based uncertainty and sensitivity analyses have been carried out as part of the YM 2008 PA.

The performance of these uncertainty and sensitivity analyses has a number of benefits, including: (i) requiring analysts to objectively confront the uncertainty present in the models that they developed and/or use, (ii) providing a rigorously derived assessment of the uncertainty present in analysis results, (iii) providing insights into the relationships between uncertainty in individual analysis inputs and the uncertainty in analysis results, (iv) providing guidance to the most appropriate areas in which to invest future research efforts, (v) extensively exercising the models in use and thereby contributing to analysis verification, (vi) aiding decision makers by explicitly representing the uncertainty in the results that underlie their decisions, and (vii) enhancing the overall credibility of the analysis.

A following presentation provides additional uncertainty and sensitivity analysis results involving expected dose to the RMEI [6]. Further, full details of the

uncertainty and sensitivity analyses performed as part of the YM 2008 PA are presented in Apps. J and K of Ref. [2].

ACKNOWLEDGMENTS

Work performed at Sandia National Laboratories (SNL), which is a multiprogram laboratory operated by Sandia Corporation, a Lockheed Martin Company, for the U.S. Department of Energy's National Nuclear Security Administration under Contract No. DE-AC04-94AL85000. Review at SNL provided by ???? and ????.

REFERENCES

1. HELTON JC et al. Yucca Mountain 2008 Performance Assessment: Conceptual Structure and Computational Implementation. *These Proceedings* 2008.
2. SANDIA NATIONAL LABORATORIES. *Total System Performance Assessment Model/Analysis for the License Application*.MDL-WIS-PA-000005 REV00, Vols. AD 01.Albuquerque, NM: Sandia National Laboratories 2008.
3. MACKINNON RJ et al. Yucca Mountain 2008 Performance Assessment: Modeling the Engineered Barrier System. *These Proceedings* 2008.
4. MATTIE PD et al. Yucca Mountain 2008 Performance Assessment: Modeling the Natural System. *These Proceedings* 2008.
5. SEVOUGIAN SD et al. Yucca Mountain 2008 Performance Assessment: Modeling Disruptive Events and Early Failures. *These Proceedings* 2008.
6. HANSEN CW et al. Yucca Mountain 2008 Performance Assessment: Uncertainty and Sensitivity Analysis for Expected Dose. *These Proceedings* 2008.
7. HELTON JC, DAVIS FJ. Latin Hypercube Sampling and the Propagation of Uncertainty in Analyses of Complex Systems. *Reliability Engineering and System Safety* 2003;81(1):23-69.
8. MCKAY MD et al. A Comparison of Three Methods for Selecting Values of Input Variables in the Analysis of Output from a Computer Code. *Technometrics* 1979;21(2):239-245.
9. HELTON JC et al. Survey of Sampling-Based Methods for Uncertainty and Sensitivity Analysis. *Reliability Engineering and System Safety* 2006;91(10-11):1175-1209.